Received: 18 December 2020 | Revised: 21 February 2021 | Accepted: 23 February 2021
DOI: 10.22034/ecc.2021.269256.1126
Eurasian Chemical Communications
SAMI

FULL PAPER

Nanocarbon-assisted biosensor for diagnosis of exhaled biomarkers of lung cancer: DFT approach

Mahmoud Mirzaei[a,*] |Oğuz Gülseren[b] |Mohammad Rafienia[a] |Amirhossein Zare[c]

[a]*Biosensor Research Center, School of Advanced Technologies in Medicine, Isfahan University of Medical Sciences, Isfahan, Iran*

[b]*Department of Physics, Bilkent University, Ankara, Turkey*

[c]*Isfahan Pharmacy Students' Research Committee, School of Pharmacy and Pharmaceutical Sciences, Isfahan University of Medical Sciences, Isfahan, Iran*

***Corresponding Author:**
Mahmoud Mirzaei
Email: mdmirzaei@pharm.mui.ac.ir
Tel.: +989034073500

Density functional theory (DFT) calculations were performed to investigate a nanocarbon-assisted biosensor for diagnosis of exhaled biomarkers of lung cancer. To this aim, an oxidized model of C_{20} fullerene (OC) was chosen as the surface for adsorbing each of five remarkable volatile organic compounds (VOC) biomarkers including hydrogen cyanide, methanol, methyl cyanide, isoprene, and 1-propanol designated by B1-B5. Geometries of the models were first optimized to achieve the minimum energy structures to be involved in further optimization of B@OC bi-molecular complexes. The relaxation of B counterparts at the surface of OC provided insightful information for capability of the investigated system for possible diagnosis of such biomarkers. In this case, B1 was placed at the highest rank of adsorption to make the strongest B1@OC complex among others whereas the weakest complex was seen for B4@OC complex. The achievement was very much important for differential detection of each of VOC biomarkers by the investigated OC nanocarbon. Moreover, the recorded infrared spectra indicated that the complexes could be very well recognized in complex forms and also among other complexes. As a final remark, such proposed nanocarbon-assisted biosensor could work for diagnosis of remarkable VOC biomarkers of lung cancer.

KEYWORDS

Nanocarbon; biomarker; exhaled; volatile organic compound; lung cancer; DFT.

Introduction

Cancer is almost the most serious problem of human health systems, which has claimed continued numerous victims without any certain treatment [1,2]. At times prevention and some other times early detection have been seen the most useful techniques regarding health protocols against the mysterious cancer [3,4]. Life styles are very much important for the case of prevention and developing accurate biosensors are highly important for early detection of cancer [5,6]. Different types of cancers have both common and different biomarkers based on the physiological actions in body; their detection is at the highest importance not to allow the cancer for more development and to employ proper medical care for the cancerous patient [7, 8]. Previous works indicated that some of volatile organic compounds (VOC) could work as exhaled biomarkers of cancer in addition to those expressed or overexpressed biomolecules into blood or any other tissue [9]. Invasive methods are sometimes used in the case of detection of those expressed biomolecules, which are somehow painful for the patients in addition to other harmful effects [10]. Moreover, due to complexity of blood and any tissue with so many types of other biological interferers or low

concentration of desired biomarker, the detection methods are not always successful especially for the case of early detection [11]. Therefore, detection of exhaled VOC biomarkers could help for early detection purpose of cancer in a non-invasive mode [12].

Lung cancer is one of the most frequent types of cancer with variable dangerous effects on the health of patients [13, 14]. Misunderstanding in early stages symptoms and lack of efficient devices for such early detection leads to diagnose of lung cancer in upper stages with serious physiological symptoms [15]. In this case, medical treatments fail to help the cancerous patient to survive and the rate of death is considerable for such patients [16]. Therefore, using novel materials and technologies are crucial for the purpose of efficient detection of lung cancer biomarkers. VOC are those exhaled biomarkers of lung cancer, which could be detected by materials with adsorption properties as discussed by earlier works [17]. Nanostructures are among those materials with potency of adsorption of gases and such VOC counterparts [18]. The surface of nanostructures could work as an adsorbent to adsorb specifically other substances in both chemical and physical modes [19-23]. Therefore, it is important to examine such capability for the purpose of VOC biomarkers detection [24]. Earlier works reported the advantage of nanostructures for adsorption of several biological and organic molecules in different fields of drug design and development in addition to biosensors [25, 26]. The idea could be very well developed in the computer-based *in silico* work avoiding external interferers [27]. In this case, molecular scale systems could be very well examined according to physicochemical aspects and mathematical algorithm search to provide insightful information for the matters at the lowest possible scale [28-31].

Within this work, a representative C_{20} nanocarbon fullerene was investigated for adsorption of already reported five typical VOC of exhaled lung cancer biomarkers (Figures 1-3). To activate the surface, the original C_{20} was functionalized by an epoxy group to make OC_{20} (OC) nanostructure for the adsorption purpose (Figure 1). It is important to note that the nanostructures could be modified by functional groups for showing more specific properties, in which the oxidation process is very much common for the purpose. Since the hydrophobic interactions are always available among the nanocarbon materials, they are usually aggregated preventing them to work very well in different media. Therefore, such oxidization could help them to stand somehow far from each other as more single-standing particles. Several efforts have been already done to make such doped or functionalized nanostructures for different purposes [32]. In this work, such oxidization was done for the investigated C_{20} nanocarbon to interact better with the external VOC biomarkers. Five remarkable VOC were already reported including hydrogen cyanide, methanol, methyl cyanide, isoprene, and 1-propanol to significantly work as exhaled biomarkers of lung cancer indicated by B1-B5 in Figure 2 [33]. The adsorption process was investigated for each of the VOC counterparts at the surface of OC. Accordingly, the idea of developing nanocarbon-assisted biosensor for diagnosis of exhaled biomarkers of lung cancer made sense (Figure 3). The idea was examined employing the advantageous computer-based quantum chemical calculations to achieve the purpose of this work.

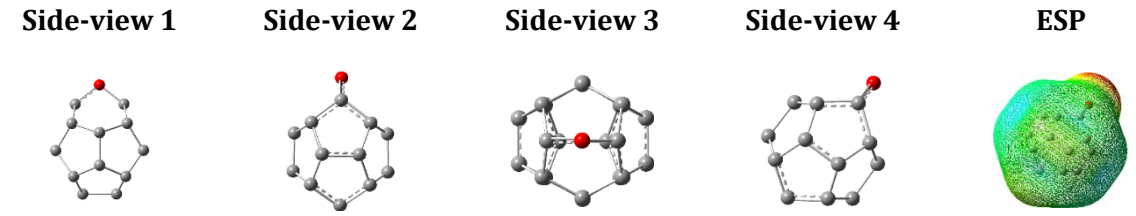

FIGURE 1 Different side-views and ESP of singular OC

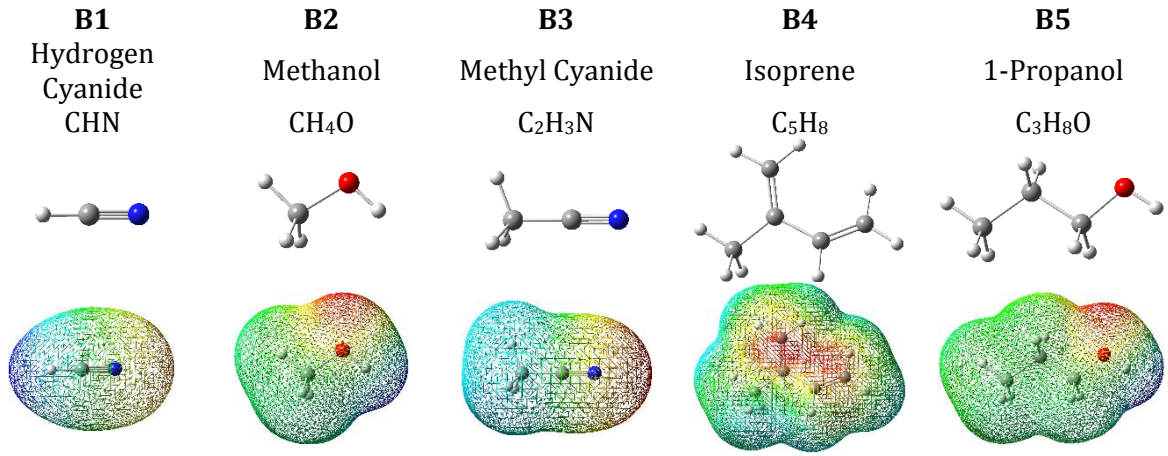

FIGURE 2 Molecular representation and ESP for five remarkable VOC biomarkers; B1-B5

Computational details

The representative model of nanocarbon was prepared by addition of epoxy group to C_{20} fullerene nanostructure (OC) (Figure 1) and allowing the structural geometries to relax during the optimization process to reach the minim energy structure. Next, five remarkable VOC exhaled biomarkers of lung cancer including hydrogen cyanide (**B1**, CHN), methanol (**B2**, CH_4O), methyl cyanide (**B3**, C_2H_3N), isoprene (**B4**, C_5H_8), and 1-propanol (**B5**, C_3H_8O) were prepared (Figure 2) and their geometries were optimized either to achieve the minimum energy structures. By obtaining all optimized singular strictures, their interacting modes were examined by locating each of the biomarkers at the surface of OC to see the best localization of such substance at the nanocarbon surface. All such bi-molecular structures were optimized to obtain the interacting B@OC complex systems (Figure 3) for further discussion of the investigated problem. Global minimum of all singular and bi-molecular structures was confirmed by performing frequency calculations for the optimized structures to avoid the existence of any imaginary frequency in addition to evaluating vibrational infrared spectra (Figure 4). Moreover, molecular orbital properties of the highest occupied and the lowest unoccupied levels (HOMO and LUMO), dipole moment (DM), and electrostatic potential (ESP) surfaces were evaluated for all the optimized singular and bi-molecular structures (Figures 1-3). All the computer-based quantum chemical calculation of this work was performed at the B3LYP exchange-correlation functional and the 6-31G* standard basis set of density functional theory (DFT) approach as implemented in the Gaussian program [34]. Indeed, it is important to use standard methods for computations to avoid uncertainty for the computed results. All the obtained calculated results of this were summered in Table 1 and Figures 1-4.

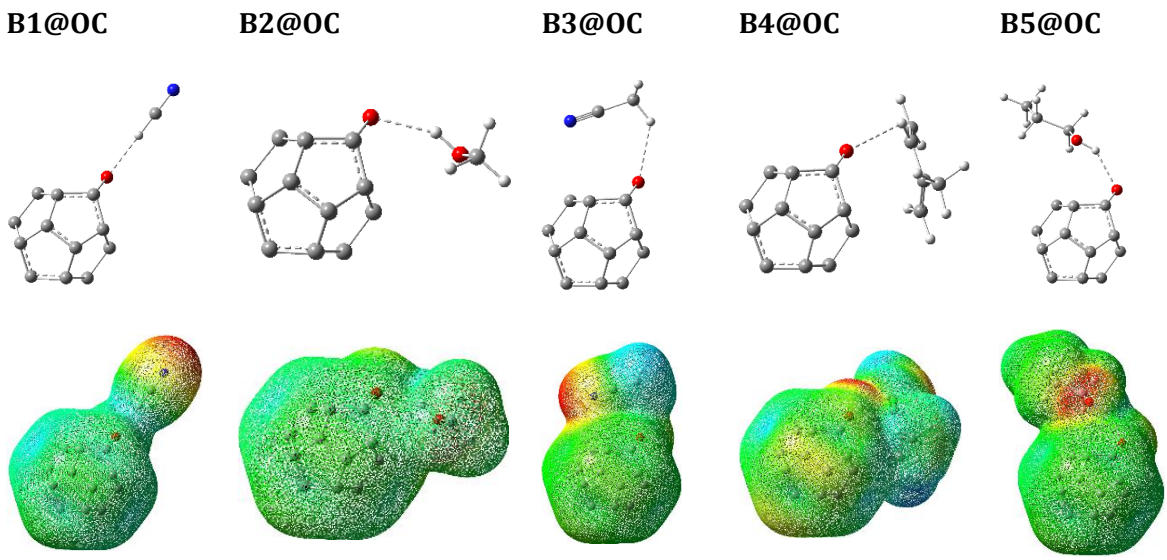

FIGURE 3 Molecular representation and ESP of bi-molecular interacting complexes of B@OC

Results and discussion

Within this work, a nanocarbon-assisted biosensor for diagnosis of exhaled biomarkers of lung cancer was investigated based on DFT calculations. Representative OC nanocarbon (Figure 1) and five typical VOC exhaled biomarkers, B1-B5, (Figure 2) were investigated to achieve the purpose of diagnosis by bi-molecular formation of B@OC interacting complexes (Figure 3). To this aim, singular and bi-molecular structures were all optimized to obtain the minimum geometries in addition to other numerical and graphical molecular properties.

TABLE 1 Obtained molecular properties for the optimized models*

Model	HOMO eV	LUMO eV	DM Debye	ID Å	BE eV
OC	-5.380	-3.260	0.407	N/A	N/A
B1	-9.773	0.556	2.905	N/A	N/A
B2	-7.198	2.048	1.694	N/A	N/A
B3	-8.882	0.995	3.814	N/A	N/A
B4	-6.184	-0.414	0.385	N/A	N/A
B5	-7.114	2.114	1.489	N/A	N/A
B1@OC	-5.718	-3.626	4.981	2.053	-0.294
B2@OC	-5.466	-3.356	1.555	1.986	-0.284
B3@OC	-5.303	-3.182	2.919	2.432	-0.219
B4@OC	-5.227	-3.126	0.767	2.628	-0.174
B5@OC	-5.445	-3.335	1.332	2.006	-0.275

*See Figures 1-3 for the models. HOMO: the highest occupied molecular orbital, LUMO: the lowest unoccupied molecular orbital, DM: dipole moment, ID: interacting distance, BE: binding energy of B and OC of B@OC complex system.

Optimized structures and molecular properties

All geometries of singular models of OC (Figure 1) and B1-B5 (Figure 2) were first optimized to achieve the minimum energy structures, all of which were confirmed by vibrational calculations to avoid the existence of imaginary frequencies. Next, bi-molecular

models of each of B1-B5 and OC were optimized to achieve the interacting B@OC complex systems (Figure 3). Both B and OC counterparts were allowed to relax during bi-molecular optimization processes, in which the results indicated the best localization of interacting molecules versus each other. It is worth to note that advantage of using C_{20} structure is experimentally availability, which helps to perform computations for the real systems [35]. Comparing interaction distances (ID) values of Table 1 could indicate different distances for such systems in addition to the unique configuration of each of B molecules at the surface of OC (Figure 3). In the case of working with small molecules, the problem of their localization at the surface is more serious because of their geometrical flexibility. However, the best localization of each of B1-B5 at the surface of OC was finally obtained by full optimization and the optimized bi-molecular complex systems were exhibited in Figure 3. The results indicated that all of these VOC biomarkers could be adsorbed with the OC surface but with different strengths designated by binding energy (BE). From Table 1, the strongest interacting bi-molecular models was seen for B1@OC and the weakest one was seen for B4@OC. As an important point, it could be mentioned that all the typical biomarkers were adsorbed at the OC surface but with more or less strength for each B counterpart. Additionally, the values of ID are in the range of physical interactions for all of B@OC bi-molecular complex systems. Comparing these results with other relative works in the literature [36], could approve the capability of such supposed OC nanocarbon for diagnosis of VOC biomarkers. In addition to optimized geometries, further calculations were performed to evaluate molecular orbital properties. Each of HOMO and LUMO energy levels could indicate the tendency of a molecule for contributing to electron transfer systems, in which different levels were detected for the singular models referring their different activities in the interacting situations. Comparing the values of HOMO for B1 (-9.773 eV) and OC (-5.380 eV) could indicate the highest favorability of B1@OC formation in all other B@OC models, in which their differences were lower than the mentioned case. Indeed, this is an in-direct interpretation and the direct interpretation should focus on the value of LUMO for OC (-3.260 eV). Additionally, the values of HOMO for B4 (-6.184 eV) and OC could indicate the lowest favorability of B4@OC complex formation. The obtained results of HOMO levels were in good agreement with those of BE values, in which the strongest and weakest complexes were detected to be B1@OC and B4@OC. The trends of molecular descriptors for defining functions of matters are obvious in such case of comparison and agreement of an original molecular feature (HOMO) and a corresponding function (BE). As a results, electron transfer between B1 and OC would be very much facile for the purpose of interactions, in which such electron would be transferred from HOMO of B1 to LUMO of OC. By formation of B@OC complex systems, the values of HOMO and LUMO were modulated regarding the interacting molecules, in which typical values were seen for B1@OC (HOMO = -5.718 eV and LUMO = -3.626 eV) as the distinguished complex of this work. Further analyses of molecular properties were done by obtaining the values of dipole moment (DM) showing the charge distributions of molecules. One important point is about zero-value of DM for original C_{20}, in which the value was increased in the OC model up to 0.407 Debye. The importance of this point is because of aggregation behaviors of nanocarbon materials, in which they could be somehow neglected by oxidization process. Typical values of DM were seen for the distinguished B1@OC and B4@OC models among other B@OC complex models. Graphical representations of electrostatic potential (ESP) surfaces could also provide the complex formations for all of B@OC bi-molecular complex systems. As concluding remarks of

this part, it could be claimed that the investigated OC model could work as a representative nanocarbon for adsorption of VOC biomarkers with different strength to show the advantage of differential detection for such systems.

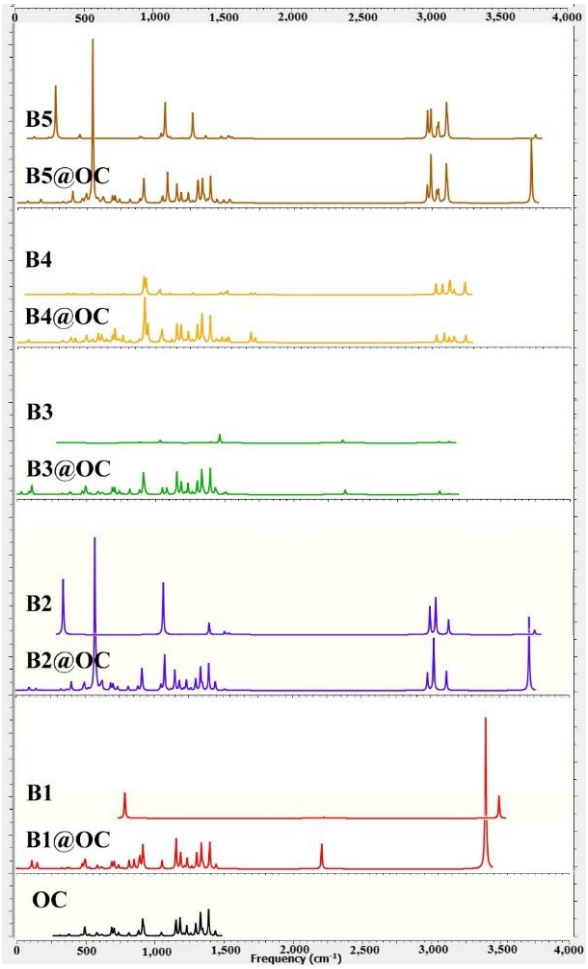

FIGURE 4 Infrared spectra of the optimized models

Infrared spectra for the optimized models

The results of previous section indicated the formation possibility for B@OC bi-molecular interacting complexes. However, providing elements for detection of such complexes is another important task. Infrared spectroscopy is an important facility for recognition of structures especially based on the functional groups. In this work, such spectra for all models (Figure 4) were evaluated to make sense of the adsorption process of each of VOC biomarkers at the surface of OC model. Comparing the spectra for isolated and bi-molecular models could approve the formation of B@OC complexes. Moreover, the strength of such complex formation could be accounted for by the magnitude of deviation of spectra of bimolecular system in comparison with each of singular B and OC models. Hence, detection of complex formations could be employed according to such infrared spectra recording.

Conclusion

In this study, the idea of nanocarbon-assisted biosensor for diagnosis of exhaled biomarkers of lung cancer was investigated by DFT calculations. The representative OC nanocarbon was put as the surface for adsorption of five typical VOC biomarkers of lung cancer. The results indicated that the

formation of B@OC bi-molecular complexes was possible with differential detection option as could be seen by different strength of complexes. Further results of energies and molecular orbital levels indicated the formation of B1@OC at the highest favorability among all of five complex systems. Additionally, recorded infrared spectra showed that the proposed differential detection could be done for the complex models besides the characteristic features of each of singular and related systems. As the final remark, the investigated OC nanocarbon could work for possible diagnosis of exhaled biomarkers of lung cancer.

Acknowledgements

The support of this work by the research council of Isfahan University of Medical Sciences under grant number 298097 is acknowledged.

Orcid:

Mahmoud Mirzaei: *https://orcid.org/0000-0001-9346-4901*

Oğuz Gülseren: *https://orcid.org/0000-0002-7632-0954*

Mohammad Rafienia: *https://orcid.org/0000-0001-6030-5082*

Amirhossein Zare: *https://orcid.org/0000-0003-3365-5591*

References

[1] C. Santucci, G. Carioli, P. Bertuccio, M. Malvezzi, U. Pastorino, P. Boffetta, E. Negri, C. Bosetti, C. La Vecchia, *Eur. J. Cancer Prev.,* **2020,** *29,* 367-81.

[2] L. Liang, L. Qili, W. Jun, Y. Yan, L. Hui, Y. Jie, *GMJ Medicine,* **2019,** *3,* 99-104.

[3] K. Akhtar, A.W. Baloch, A. Kurmashvili, *GMJ Medicine,* **2018,** *2,* 65-71.

[4] X. Chen, J. Gole, A. Gore, Q. He, M. Lu, J. Min, Z. Yuan, X. Yang, Y. Jiang, T. Zhang, C. Suo. *Nat. Commun.,* **2020,** *11,* 1-10.

[5] V. Perduca, H. Omichessan, L. Baglietto, G. Severi, *Curr. Opin. Oncol.,* **2018**, *30,* 61-67.

[6] G. Yang, Z. Xiao, C. Tang, Y. Deng, H. Huang, Z. He, *Biosens. Bioelectron.,* **2019**, *141,* 111416.

[7] V.S. Jayanthi, A.B. Das, U. Saxena, *Biosens. Bioelectron.,* **2017**, *91,* 15-23.

[8] M. Moghaddaszadeh, L. Fahmideh, B. Fazeli-Nasab, *J. Plant Bioinform. Biotech.*, **2021**, *1,* 25-38.

[9] Z. Jia, A. Patra, V.K. Kutty, T. Venkatesan, *Metabolites,* **2019**, *9,* 54-70.

[10] V.H. Teixeira, C.P. Pipinikas, A. Pennycuick, H. Lee-Six, D. Chandrasekharan, J. Beane, T.J. Morris, A. Karpathakis, A. Feber, C.E. Breeze, P. Ntolios, *Nat. Med.*, **2019**, *25,* 517-525.

[11] F.R. Hirsch, W.A. Franklin, A.F. Gazdar, P.A. Bunn, *Clin. Cancer Re.,* **2001**, *7,* 5-22.

[12] R. Becker, *Med. Hypotheses,* **2020**, *143,* 110060.

[13] J.D. Minna, J.A. Roth, A.F. Gazdar, *Cancer Cell.,* **2002**, *1,* 49-52.

[14] D. Hammoudi, A. Sanyaolu, D. Adofo, I. Antoine, *GMJ Medicine,* **2017**, *1,* 3-8.

[15] W.D. Travis, *Clin. Chest Med.,* **2002**, *23,* 65-81.

[16] S.A. Murray, K. Boyd, M. Kendall, *BMJ: British Medical Journal,* **2002**, *325,* 929-932.

[17] F.L. Liu, P. Xiao, H.L. Fang, H.F. Dai, L. Qiao, Y.H. Zhang, *Physica. E.,* **2011**, *44,* 367-372.

[18] Q. Wan, Y. Xu, X. Chen, H. Xiao, *Mol. Phys.,* **2018**, *116,* 2205-2212.

[19] S. Ariaei, *Lab-in-Silico.,* **2020**, *1,* 44-49.

[20] R. Faramarzi, M. Falahati, M. Mirzaei, *Adv. J. Sci. Eng.,* **2020**, *1,* 62-66.

[21] K. Harismah, O.M. Ozkendir, M. Mirzaei, *Adv. J. Sci. Eng.,* **2020**, *1,* 74-79.

[22] O.M. Ozkendir, *Adv. J. Sci. Eng.,* **2020**, *1,* 7-11.

[23] M. Afshar, R. Ranjineh Khojasteh, R. Ahmadi, *Eurasian Chem. Commun.,* **2020**, *2,* 595-603.

[24] V. Nagarajan, R. Chandiramouli, *Comput. Theor. Chem.,* **2018**, *1138,* 107-116.

[25] E. Tahmasebi, E. Shakerzadeh, *Lab-in-Silico.,* **2020**, *1,* 16-20.

[26] M. Mirzaei, H.R. Kalhor, N.L. Hadipour, *J. Mol. Model.,* **2011**, *17,* 695-699.

[27] M. Mirzaei, *Lab-in-Silico.,* **2020**, *1,* 31-32.
[28] H. Agil, N. Akduran, *Adv. J. Sci. Eng.,* **2020**, *1,* 122-127.
[29] M. Mirzaei, *Adv. J. Sci. Eng.,* **2020**, *1,* 1-2.
[30] S. Ariaei, H. Basiri, M. Ramezani, *Adv. J. Chem. B,* **2020**, *2,* 18-25.
[31] O.M. Ozkendir, *Lab-in-Silico.,* **2020**, 1, 33-37.
[32] S. Gunaydin, O.M. Ozkendir, *Lab-in-Silico.,* **2020**, *1,* 56-60.
[33] Y. Sakumura, Y. Koyama, H. Tokutake, T. Hida, K. Sato, T. Itoh, T. Akamatsu, W. Shin, *Sensors,* **2017**, *17,* 287-299.
[34] M.J. Frisch, G.W. Trucks, H.B. Schlegel, G.E. Scuseria, M.A. Robb, J.R. Cheeseman, G. Scalmani, V. Barone, B. Mennucci, G.A. Petersson, H. Nakatsuji, M. Caricato, X. Li, H.P. Hratchian, A.F. Izmaylov, J. Bloino, G. Zheng, J.L. Sonnenberg, M. Hada, M. Ehara, K. Toyota, R. Fukuda, J. Hasegawa, M. Ishida, T. Nakajima, Y. Honda, O. Kitao, H. Nakai, T. Vreven, J.A. Montgomery, Jr., J.E. Peralta, F. Ogliaro, M. Bearpark, J.J. Heyd, E. Brothers, K.N. Kudin, V.N. Staroverov, R. Kobayashi, J. Normand, K. Raghavachari, A. Rendell, J.C. Burant, S.S. Iyengar, J. Tomasi, M. Cossi, N. Rega, J.M. Millam, M. Klene, J.E. Knox, J.B. Cross, V. Bakken, C. Adamo, J. Jaramillo, R. Gomperts, R.E. Stratmann, O. Yazyev, A.J. Austin, R. Cammi, C. Pomelli, J.W. Ochterski, R.L. Martin, K. Morokuma, V.G. Zakrzewski, G.A. Voth, P. Salvador, J.J. Dannenberg, S. Dapprich, A.D. Daniels, O. Farkas, J.B. Foresman, J.V. Ortiz, J. Cioslowski, D.J. Fox, *Gaussian, Inc., Wallingford CT,* **2009**.
[35] Z. Wang, X. Ke, Z. Zhu, F. Zhu, M. Ruan, H. Chen, R. Huang, L. Zheng, *Physics Letters A.,* **2001**, *280,* 351-356.
[36] R. Majidi, M. Nadafan, *Physics Letters A.,* **2020**, *384,* 126036.

How to cite this article: Mahmoud Mirzaei*, Oğuz Gülseren, Mohammad Rafienia, Amirhossein Zare. Nanocarbon-assisted biosensor for diagnosis of exhaled biomarkers of lung cancer: DFT approach. *Eurasian Chemical Communications*, 2021, 3(3), 154-161. **Link:** http://www.echemcom.com/article_126932.html